12TH CANADIAN CONFERENCE ON EARTHQUAKE ENGINEERING
JUNE 17-20, 2019
CHÂTEAU FRONTENAC
QUÉBEC, QC.
12ÈME CONFÉRENCE CANADIENNE DU GÉNIE PARASISMIQUE
17-20 JUIN 2019
CCEE 2019

Damage assessment of an RC low-rise building structure having torsional irregularity at the ground story in the M_w 5.4 15 November 2017 Pohang earthquake in Korea

Han-Seon Lee[1] and Huiling Piao[2]

[1] Professor, School of Civil, Environmental, and Architectural Engineering, Korea University
[2] Graduate Student, School of Civil, Environmental, and Architectural Engineering, Korea University

ABSTRACT

The 15 November 2017 M_w=5.4 Pohang earthquake caused severe damages on approximately two thousand buildings in Korea. The most severely damaged buildings among them are RC low-rise piloti-type building structures with the number of stories less than or equal to five. A 4-story RC piloti-type residential building having high degree of soft/weak story, torsional irregularities at the ground story and located 3.2km from the epicenter is selected as the representative structure. This study investigates the mechanism of the damages in this 4-story building structure based on the post-earthquake observations and on the results of nonlinear analyses by PERFORM-3D. Shear demands in columns exceed the shear capacities given by concrete, V_c, which means the failure of column, because V_s contributed by steel cannot be relied on due to the large spacings of transverse reinforcements and the non-seismic hooks. The initial elastic response was governed by the third torsional mode, with the period of 0.2s, and then after the shear failure of flexible frames, the mode changed to the translation-torsion coupled mode with the period of 0.550s elongated from the elastic fundamental period of 0.339s. Though the maximum drift in the flexible side, 19.6mm (0.61%), is not considered to be serious from the viewpoint of high-seismicity region, this study shows that this drift can cause the failure of the structures in the low- to moderate seismic regions, such as Korea.

Keywords: Pohang earthquake, piloti-type structures, torsional irregularity, damage assessment, numerical simulation.

INTRODUCTION

Recent history of earthquakes in Korean Peninsula and Korean seismic design codes

The Korean Peninsula is located on the far-eastern Eurasian plate (Figure 1(a)), and generally considered to be stable with low to moderate intraplate seismic activity, but the historical seismicity of this region indicates large secular variations in earthquake rate and energy release[1]. The seismic design code for building structures in Korea was introduced for the first time in 1988 and modified in 1995, 2005, 2015 and 2017. A large portion of the Korean seismic design code has been derived from the UBC (Uniform Building Code) and IBC (International Building Code) developed in high seismicity regions, because of the lack of information on the ground motion records to establish such seismic design codes and the actual damages of structures due to these earthquakes. Since the seismic behavior of structures may be quite different between high and low seismic regions, the design codes developed for high seismicity may not be adequate for the application to the structures in the low seismic region such as Korea[2].

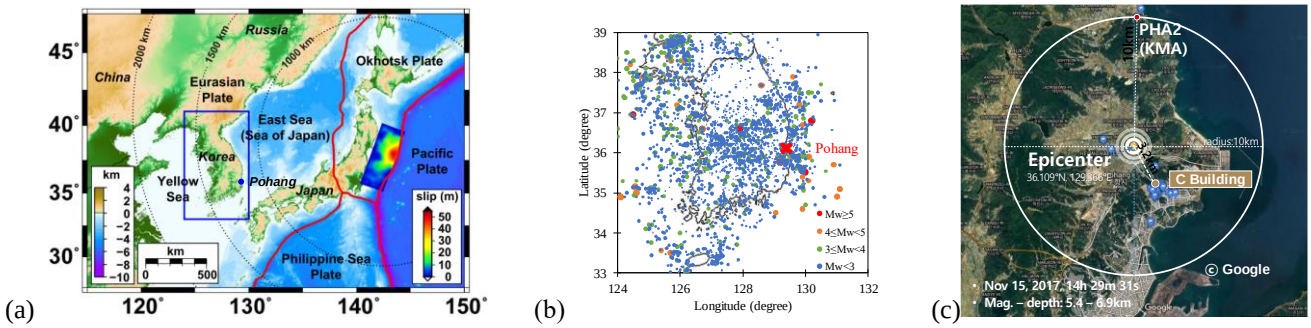

Figure 1. Instrumantal tectonic plates and earthquakes in Korean Peninsula: (a) location of Korean Peninsula, (b) earthquake epicenters and recorded by instruments since 1978[3], (c) location of epicenter and the location of target building for simulation.

The Korean seismic instrumental recording began in 1978, the instrumentally recorded earthquakes include ten events with magnitudes greater than or equal to 5.0 as shown in Figure 1(b). The short history of instrumental seismic observation in the Korean Peninsula may not be enough for inference of earthquakes with long recurrence intervals of thousands of years.

M_w=5.4, 15 Nov. 2017, Pohang earthquake

On 15 November 2017, Pohang Earthquake with M_w=5.4, hereafter will be called just Pohang earthquake, occurred in a hypocentral depth of 3~7km in the city, Pohang in Figure 1(c). The slope of the fault plane is northwestward and shows the movement of the downward oblique direction fault. A total of 1,350 aftershock earthquakes occurred between 15 Nov. 2017 and 28 Feb. 2018, with the main distribution in the northeast-southwest direction and the hypocentral depth is around 4km[4]. This earthquake was one of the largest and most damaging events since the first seismograph was installed in 1905, and the second-largest in magnitude since 1978 when scientific instrumental observations began[5]. It caused 92 injuries and severe damages on residential buildings with an estimated economic loss of US$52 million[6].

Figure 2(a) shows the response spectra of the ground accelerograms (E-W, N-S, U-D) recorded at the Station PHA2 with the location in Figure 1(c), where the strong motions occurred from 3s to 10s and the peak ground accelerations (PGA) are 0.25g, 0.28g and 0.13g along E-W, N-S and U-D directions, respectively, in Figure 2(b). The response spectra exceed the design spectra of KBC2016[7] around the periods of 0.1s and 0.6s. This earthquake ground motions represent the typical characteristics of moderate seismicity such as short-duration, large-amplitude acceleration in the high-frequency region, and severe damages by brittle failures on many non-ductile structures.

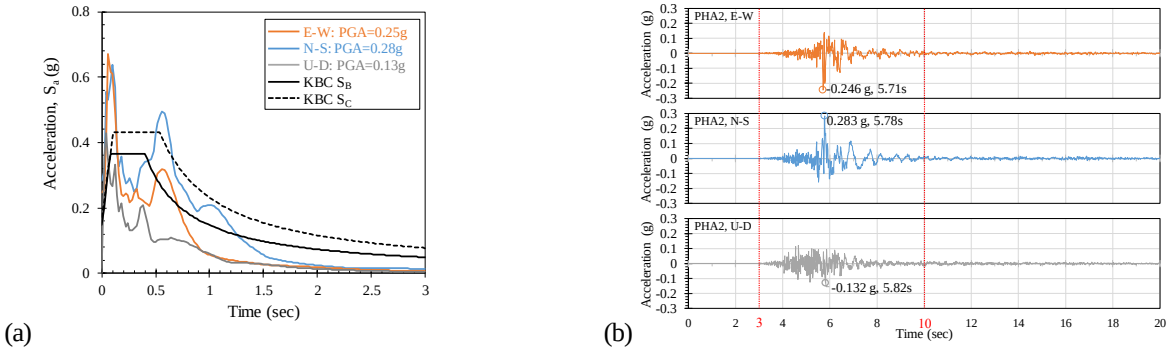

Figure 2. Recorded ground motions at the Station PHA2[8]: (a) response spectra, (b) time histories of recorded ground motions.

The so-called piloti-type structures have gained a popularity in recent years for the effective use of the ground space, and so nearly 90% of low-rise residential buildings are reported to be piloti-type as of 2015[9]**.** However, these buildings showed significant damages during the Pohang earthquake due to the high irregularities of weak/soft story and torsional irregularity at the ground story[10]. A total of 56 RC piloti-type buildings, ranging between 3- to 5-story with the height of 7.30~15.2m, and the floor area of 111~270m^2, and the aspect ratio(longer dimension/shorter one) of 1.01~2.90, are reported to have damages at 3 different levels: S(severe or collapse), M(medium) and L(light)(Tables (1) and (2))[11]. All the damaged buildings are located within 10km from the epicenter and show typical shear failures and steel bucklings in the columns and shear walls. The examples of damage levels representing "Severe(S)" and "Medium(M)" are given in Figure 3.

Figure 3. Examples of damaged structural members in 15 Nov. 2017 Pohang earthquake: (a) "Severe" damaged column, (b) "Medium" damaged column, (c) "Severe" damaged wall, (d) "Medium" damaged wall.

Table 1. Damaged piloti-type structures in Pohang earthquake

No. of structures	56	**Floor Area (m^2)**	111~270
Epicenter (*km*)	1.56~9.73	**Aspect Ratio**	1.01~2.90
Height (*m*)	7.30~15.2	**No. of Stories**	3~5

Table 2. Damage level by inspection

Damage Level	No. of structures	Ratios (%)
S	25	45
M	12	21
L	19	34
Total	56	100

NUMERICAL SIMULATION OF A DAMAGED BUILDING STRUCTURE USING MEASURED GROUND ACCELEROGRAMS AT THE STATION PHA2 IN POHANG EARTHQUAKE

Target structure – Building C

Building C, the location of which is given in Figure 1(c), is the most representative of all the damaged RC low-rise piloti-type building structure and selected as the target structure in the following assessment of earthquake damage (Figure 4). Building C constructed in 2011 should have been designed according to KBC2009[12], which is similar to IBC2005, but it did not actually conform to the seismic requirements of the code. This building represents a typical case of torsional irregularity due to the fact that the staircase is located at the corner of the floor (Figure 4(b)). The damaged two columns, C1 and C2, have the same cross section of 600×400mm (Figures 4(c)-(e)), and the diameter of the longitudinal reinforcement is 19mm. According to KBC2009, the spacing should be less than the least of $8db_l$ (diameter of longitudinal reinforcement), $24db_h$ (diameter of hoop), $0.5[\min(b_w, d)]$(width or depth of cross section) and 300mm, which is 152mm. The actual spacings of transverse reinforcements appear to be around 200mm, in addition to the omission of cross ties and the use of 90° non-seismic hooks. A rainwater pipe inside the transverse steel shown in Figure 4(d) decreased not only shear but also axial capacity of the column C1. Figure 4(f) shows shear cracks at the corner of the wall.

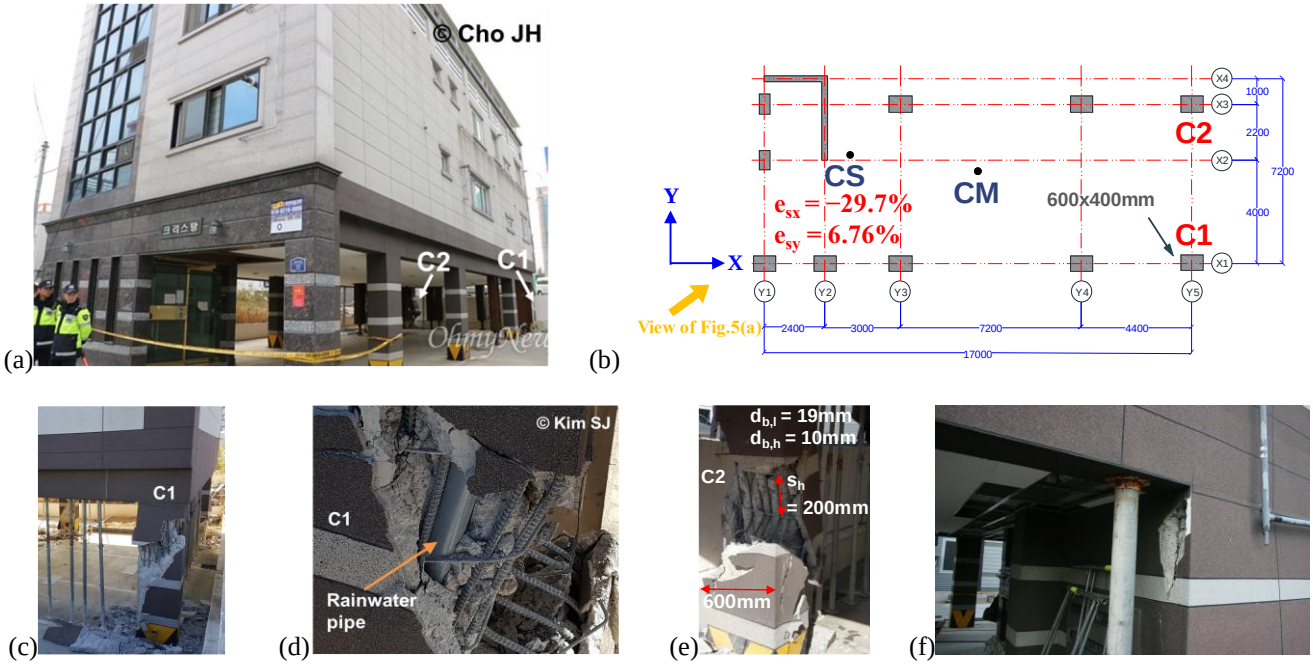

Figure 4. Target structure(Building C) in Figure 1(c): (a) Building C, (b) 1st floor plan, (c)-(e) damaged columns, (f) damaged shear wall. [13]

Though this building did not conform to the current seismic code, the design load according to KBC2009 is now given as follows for the purpose of comparison: The effective seismic weight(W) of analytical structure is set as the $1.0DL$(10,600kN). The design base shear force, V_d=933kN($0.088W$), is calculated using Equations (1) and (2), with the response modification factor R=5(building frame system with ordinary walls) and the occupancy importance factor I_E=1.0.

$$V_d = C_S W = (0.088)(10600) = 933\text{kN} \quad (1)$$

$$C_S = \frac{S_{DS}}{(R/I_E)} = \frac{0.440}{(5/1.0)} = 0.088, \text{ but not exceeding } C_S = \frac{S_{D1}}{(R/I_E)T} = \frac{0.235}{(5/1.0)0.332} = 0.142 \quad (2)$$

where C_S is the seismic coefficient; S_{DS} and S_{D1} are the design spectral accelerations at periods 0.2s and 1.0s, respectively; and T_a is the approximate fundamental period estimated using the empirical equation, $T_a = C_T h_n^{3/4} = (0.049)(12.8\text{m})^{3/4} = 0.332$s. The degree of torsional irregularity of this structure in y-direction according to the code is $\delta_{flex.}/\delta_{center}$=1.90>1.20.

Numerical model

PERFORM-3D[14] is used for the earthquake simulation of this structure. The compressive strength of concrete(f_c') is assumed to be the same as the design compressive strength, 21MPa, with the strain of 0.0025m/m at the ultimate stress, and the modified Thorenfeldt reference model is used to model the concrete by neglecting the tensile strength as shown in Figure 5(a). The yield strength of steel(f_y) is assumed to be the same as the design yield strength, 400MPa, Figure 5(b) shows the material models for reinforcements. The strength loss of steel is assumed to occur at compressive strains of 0.0055m/m due to the buckling of the long longitudinal reinforcement with the large spacing of transverse reinforcement. In Figure 5(c), the shear strength of the wall, v_n, is calculated according to ASCE/SEI 41-13[15] using the equation of yield strength, $v_n = a_s\sqrt{f_c'} + \rho_t f_y = 2.35$MPa, and the backbone curve is defined to be trilinear when the shear stress of the first point is $0.6v_n$ with the initial effective stiffness of G_{eff}=0.5G_c(G_c: shear modulus of conrete), and the second point is determined by the yield strain of ε_y = 0.004m/m.

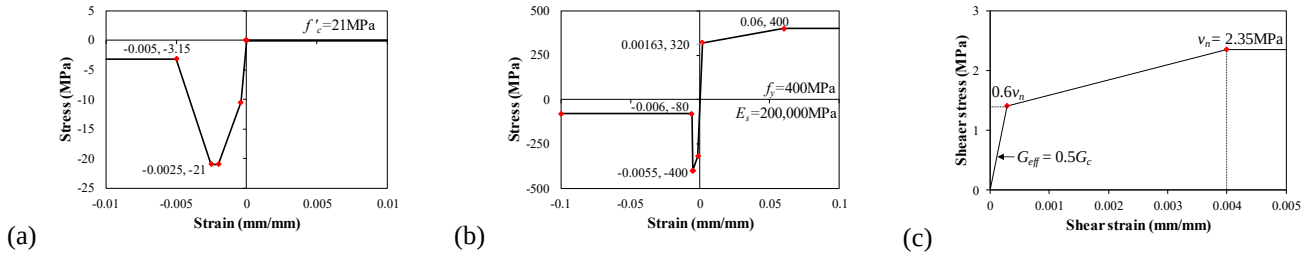

Figure 5. Stress-strain relation of material for analytical model: (a) concrete, (b) steel, (c) shear material for the wall.

Since the reinforcement details of columns did not conform to the requirements of seismic details, all the concrete in columns is assumed to be "Unconfined" (Figure 6(a)). And "Inelastic fiber section" is used for columns at the ground story (Figure 6(b)). Walls in the ground story are modeled as inelastic "Shear Wall" element which describes the axial and in-plane bending behaviors by using the inelastic fiber sections (Figure 6(d)) in the longitudinal direction, and shear behavior by defining inelastic concrete shear material as shown in Figure 5(c).

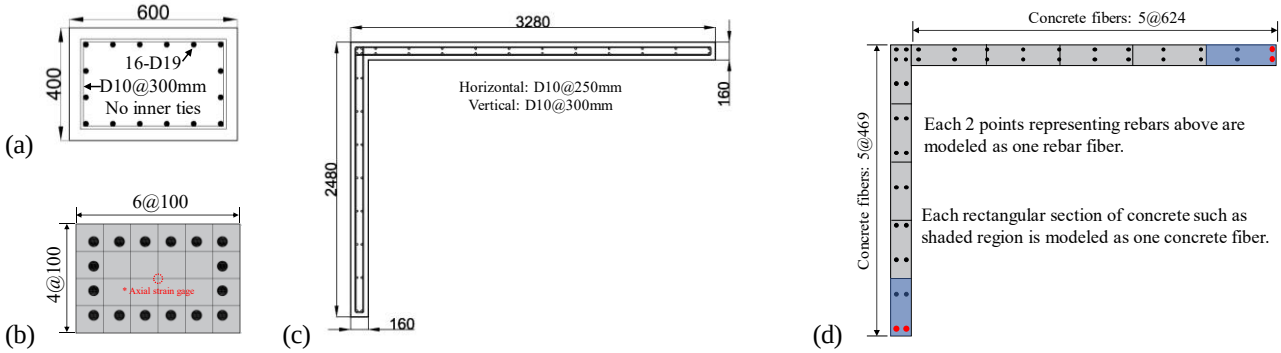

Figure 6. PERFORM-3D analytical model(mm): (a) cross section of column, (b) fiber model of column, (c) cross section of wall, (d)fiber model of wall.

Figures 7 shows the periods and the corresponding mode shapes of the structure from the modal analysis. The first mode is the coupled mode by the translational movement in y-direction and the torsion with the period of 0.339s, and the second mode is the coupled mode by the translational movement in x-direction and the torsion with the period of 0.237s, with the third mode being only the torsional movement with the period of 0.200s.

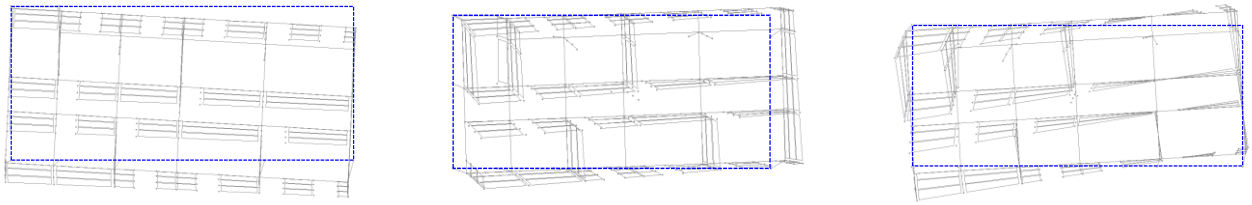

(a)T_1 = 0.339s (b)T_2 = 0.237s (c)T_3 = 0.200s

Figure 7. Natural periods and corresponding mode shapes.

Results of nonlinear analysis

Figures 8(a) and (b) give the time histories of the interstory drifts in the y-direction, δ_y, δ_{y1} and δ_{y5}, and the torsional deformation, θ_t, at the ground story, respectively. Figures 8(c) and (d) display the time histories of the base shear, V_y, of Frame Y1 and Frame Y5 in the y-direction and the base torsional moment, T_{total}. The torsional moment contributed by the x- and y-directional frames, T_x and T_y, are presented in Figures 8(e) and (f), respectively. The instants (1) and (2) represent the instants of the maximum positive and negative drifts at the flexible side, frame Y5, respectievely, with instants (3) and (4) representing the instants of the maximum positive and negative torsional deformations, respectively. In the time histories of T_{total} (Figures 8(d)), the maximum torsional moment occurs at instant (a) in the blue shaded time span A, while the maximum torsional moment T_x occurs with the opposite-directional torsional moment in the y-direction in the orange shaded time span B.

After the first significant yielding, the initial elastic fundamental period of 0.339s is elongated to the actual predominant period of 0.550s as shown in Figure 8(a). Besides, the torsional irregularity, $\delta_{y5}/\ \delta_{avg}$=19.6mm/12.1mm=1.62, is smaller than that of the elastic one, 1.90.

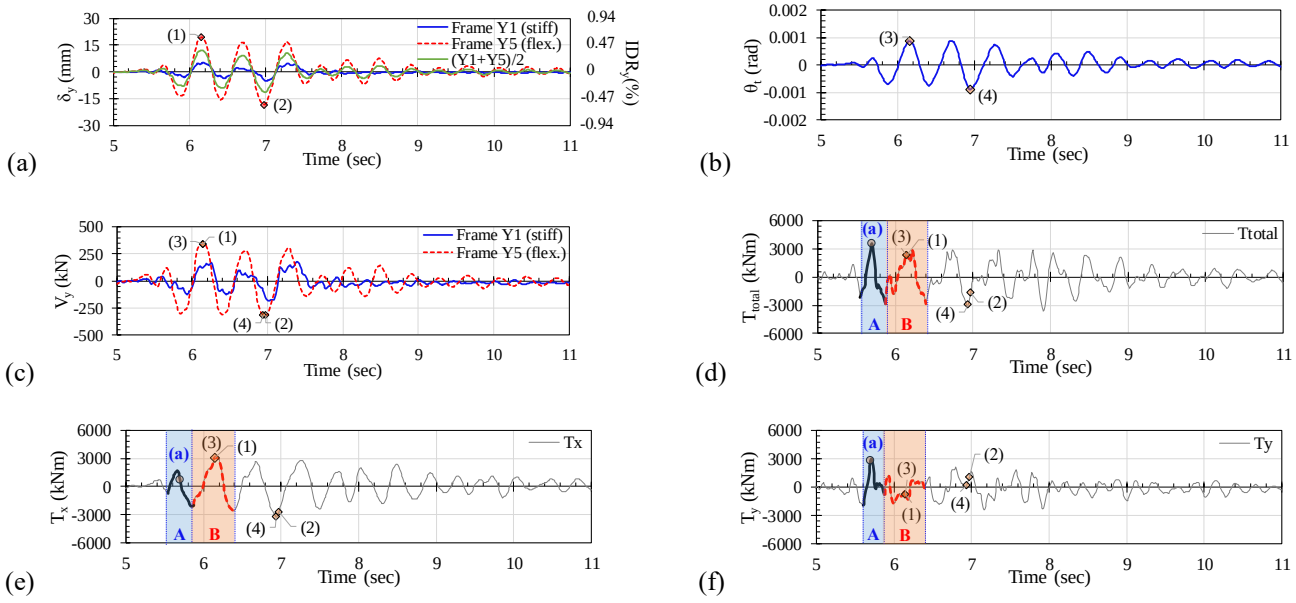

Figure 8. Time histories in the first story: (a) y-directional displacement, δ_y, (b) torsional displacement, θ_t, (c) y-directional shear force, V_y, (d-f) torsional moments: (d) T_{total}, (e) T_x and (f) T_y.

-Comparison of shear demand and capacity of column C2

The shear demand, given by the hysteretic curve of P_{C2}-$V_{y,C2}$, is compared with the shear capacities: the shear strength contributed by concrete(V_c), the nominal shear strength(V_n= V_c+ V_s) including the contribution by steel(V_s), and the shear strength corresponding to the flexural yielding at both top and bottom of column(V_{mp}), which are plotted as red dotted line, orange dotted line and black bold line, respectively, in Figure 9(a). The reliable shear capacity is considered to be equal to V_c only, since the transverse reinforcements cannot contribute the resistance due to non-seismic details. Therefore, the structure is considered to have failed in shear at instant (1), 6.15s.

In Figure 9(c), the maximum shear force, 224kN, at instant (1), 6.15s, decreases to the next peak shear force, 170kN at 7.23s, even though the axial forces are similar at these two instants in Figure 9(a). Hence, it can be inferred that shear damage happened in the column C2 during 6.15s to 7.23s. In Figure 9(a) and (b), the large variation of axial force caused by the large overturning moment is observed, and the flexural capacity of C2 is far larger than the flexural demand. Figure 9(c) shows the maximum lateral displacement, $\delta_{y,C2}$=19.6mm(0.61%) with the corresponding axial force of P_u=0.31$f_c'A_g$, and that shear stiffness in compression is relatively larger than that in tension.

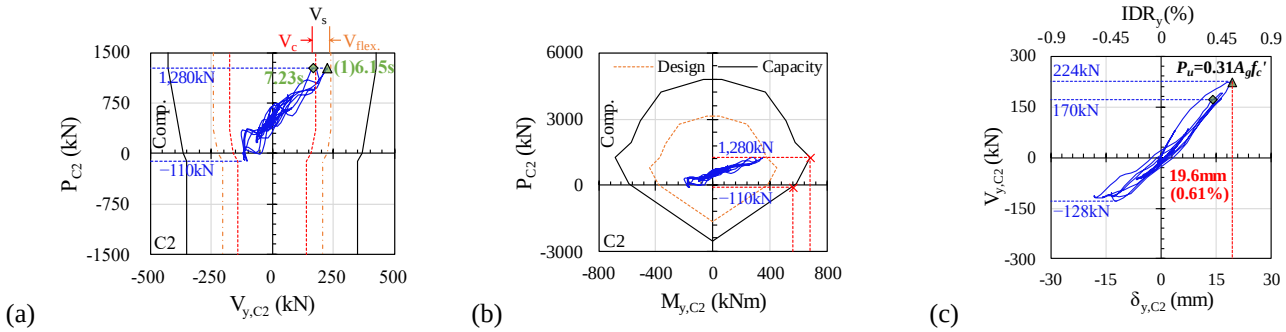

Figure 9. Hysteretic relations between: (a) P_{C2}-$V_{y,C2}$, (b) P_{C2}-$M_{y,C2}$, (c) $V_{y,C2}$-$\delta_{y,C2}$.

-Torsional resistance mechanisms

The hysteretic responses between the shear and torsion at the ground story are shown in Figure 10. The maximum demand in earthquake load is 1,510kN which is much larger than the design load given in Equation (1), 933kN. Significant inelastic response can be observed in Figure 10(a) with the maximum positive and negative central floor drift, δ_y, being 12.2mm(0.38%) and −11.5mm(−0.36%). The value of the maximum drift of the flexible frame(δ_{y5}), 19.6mm (0.61%), is much larger than that at the stiff frame(δ_{y1}), 5.13mm (0.16%), showing the more critical drift demands in the flexible side (Figure 10(b)). In Figure 10(e), in the initial stage of the earthquake, the torsional stiffness regarding T_y at instant (a) is 15,400MNm/rad, much greater than that of T_x (=4,020MNm/rad). However, at instant (1), due to the yielding of y-directional frames (Figure 10(a)), the hysteretic curve in T_y-θ_t appears to be almost horizontal, which indicates significant degradation of the stiffness. In Figure 10(f), the response curve of T_{total}-θ_t, combining the characteristics of T_x-θ_t and T_y-θ_t, are mostly governed almost by T_x-θ_t (Figure 10(d)). The slope of V_y-T_y (Figure 10(g)) represents eccentricity, e_x=T_y/V_y, less than 4.2% at instants (1)-(4). The response behavior of T_{total}-V_y (Figure 10(h)) is governed by T_x-V_y (Figure 10(g)). In Figure 10(i), the range of V_x(−1,070~1,060kN) is relatively smaller than the range of V_y(−1,560~1,550kN). Especially at instants (1)-(4), the values of V_y=−1,500~1,510kN, are much greater than the values of V_x=145~248kN.

The values of torsional moments, T_x, T_y and T_{total}, torsional deformation, θ_t, y-directional shear force, V_y, y-directional drifts, δ_{stiff} and $\delta_{flex.}$, the ratio of $\delta_{flex.}/\delta_y$ and eccentricity, e_x, at instants (a) and (1)-(4) are given in Table 3.

At instant (a) when the strong motion started the period of the third torsion mode, T_3=0.200s, is similar to that corresponding to the maximum spectral acceleration, 0.1s as given in Figure 2(a), and V_y=−183kN is small when compared to the T_{total}=3,600kNm with the large ratio of $\delta_{flex.}/\delta_y$=4.80.

The instants (1) and (2) represent the time instants of the maximum positive and negative drifts, respectively, while the instants (3) and (4) indicate the maximum positive and negative torsional deformations, respectively. At instants (1)-(4), the modal period of the elastic y-directional translation and torsion coupled mode (T_1=0.339s) in the modal analysis changed to be elongated to the period of 0.55s due to failure of columns in the flexible side.

Table 3. Forces, deformations and eccentricity.

instant	***remark***	***Time* (s)**	***T_x* (kNm)**	***T_y* (kNm)**	***T_{total}* (kNm)**	***θ_t* (rad)**	***V_y* (kN)**	***δ_{stiff}* (mm)**	***$\delta_{flex.}$* (mm)**	***δ_{flex}/δ_y***	***e_x* (%)**
(a)	$T_{total,max}$	5.70	745	2,860	3,600	0.000185	−183	−1.16	1.99	4.80	−91.9
(1)	$\delta_{flex.,max}$	6.15	3,060	−790	2,270	0.000885	1,510	4.54	19.6	1.62	−3.07
(2)	$\delta_{flex.,min}$	6.97	−2,720	1,080	−1,640	−0.000836	−1,500	−4.03	−18.3	1.64	−4.21
(3)	$\theta_{t,max}$	6.15	3,060	−790	2,270	0.000885	1,510	4.54	19.6	1.62	−3.07
(4)	$\theta_{t,min}$	6.94	−3,190	205	−2,980	−0.000889	−1,360	−2.33	−17.5	1.76	−0.89

According to Figure 10 and Table 3, the torsional resistance mechanisms can be characterized by three categories as follows:

(i) At instant (a) when the torsional mode governs, the maximum torsional moment, T_{total}=3,600kNm with the small torsional deformation, θ_t=0.000185rad, is resisted collaboratively by T_x=745kNm and T_y=2,860kNm, therefore, leading to the largest torsional stiffness, 19,400 MNm/rad.

(ii) At instant (4), T_{total}=−2,980kNm governed by T_x=−3,190kNm(≈T_{total}), with negligible T_y=205kNm≈0 and large V_y=−1,360kN causes very small eccentricity, e_x=−0.89%, but with reduced torsional stiffness in the y-direction, this torsional moments also causes large torsional deformation, θ_t=−0.000889rad.

(iii) At instants (1)-(3), T_x (3,060kNm and −2,720kNm), is 2~3 times larger than T_y (−790kNm and 1,080kNm), T_{total} is reduced by the counteraction between T_x and T_y, but still remains large. In this case, relatively large shear forces, V_y ≈1,500kN with the smaller T_y, ended up with e_x=−4.21~−3.07% as shown in Figure 10(g).

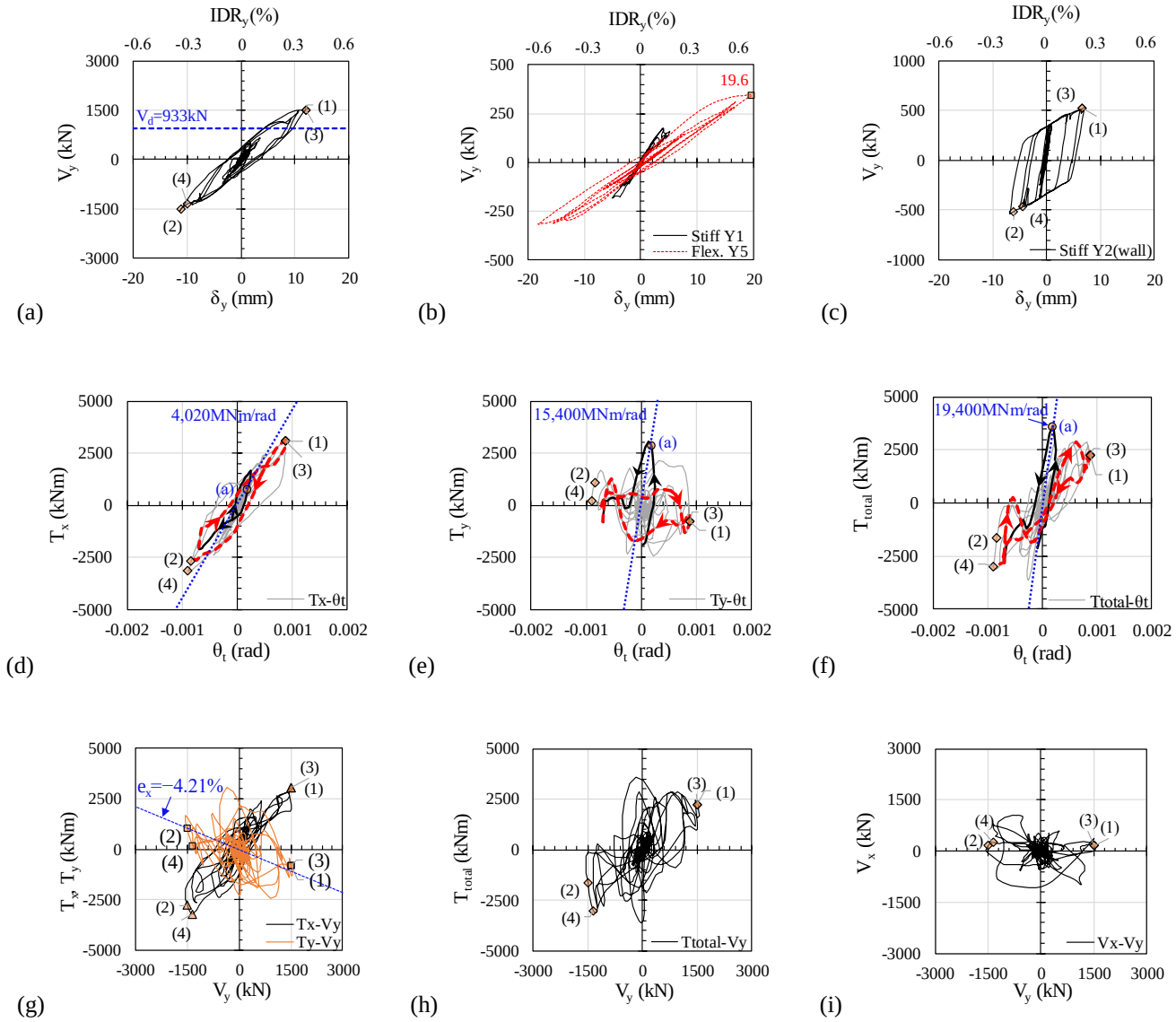

Figure 10. Seismic interaction on the ground story: (a) V_y- δ_y, (b) V_y- δ_y of the stiff(Y1) and the flexible(Y5) edges, (c) V_y- δ_y of the stiff wall(Y2), (d) T_x- θ_t, (e) T_y- θ_t, (f)T_{total}-θ_t, (g) T_x-V_y and T_y-V_y, (h) T_{total}-V_y, (i) V_x-V_y.

CONCLUSIONS

The 15 Nov. 2017, M_w=5.4 Pohang Earthquake caused severe damages on many non-seismic piloti-type reinforced concrete low-rise residential buildings in a limited range of epicentral distance (10km). This paper explains the characteristics of Pohang earthquake ground motions recorded at one station with the statistics of damaged piloti-type structures and examines the seismic behaviors of one representative target building by analytical simulation using PERFROM-3D. The followings are concluded from this study.

(1) The seismic responses of the target structure (Building C) located at the epicentral distance of 3.2km are simulated using PERFORM-3D with accelerograms recorded at the Station PHA2 located 10km from the epicenter. Because the transverse reinforcements cannot contribute the resistance due to the non-seismic details (e.g.: 90° hooks), the reliable shear capacity is considered to be equal to V_c, shear strength contributed by concrete. The fact that the shear demands in C2, given by the analytical results exceed the shear capacities, V_c, clearly manifests the occurrence of shear failure of the column in the actual building at the initial stage of earthquake ground motion.

(2) The initial elastic response was governed by the third torsional mode, with the period of 0.2s, and then after the shear failure of flexible frames, the mode changed to the translation-torsion coupled mode with the period of 0.550s elongated from the elastic fundamental period of 0.339s. At the initial response of structure, the torsion resisting mechanism in resisting the external torsional inertia moments is collaborative between the torsional moment resisted by the x-directional frames and that resisted by the y-directional frames, but changed to be counteractive each other after the occurrence of shear failure of columns in the flexible frame, leading to highly degraded torsional stiffness. The final maximum drift in the flexible side, 19.6mm (0.61%), and the torsion irregularity ratio, $\delta_{flex}/\delta_y \approx 1.6$, are not considered to be serious from the viewpoint of high-seismicity region. But in the low- to moderate-seismic regions, such as Korea, these values mean the failure of the structures.

ACKNOWLEDGMENTS

The research presented herein was supported by the National Research Foundation of Korea (NRF-2009-0078771, NRF-2016R1C1B1016653, and NRF-2017R1D1A1B03033488) and the Korea University Grant. The authors are grateful for such support.

REFERENCES

[1] Soung Eil Houng, Junghyung Lee and Tae-Kyung Hong. (2016). “Dynamic seismic response of a stable intraplate region to a megathrust earthquake”. *Tectonophysics*, 689, 67-78.

[2] Taejin Kim, Dong-Guen Lee, Hyun Ko and So-Hoon Cho. (2006). “Code Related Issues in Seismic Design of Buildings in Korea”. In *4th International Conference on Earthquake Engineering*, Taipei, Taiwan.

[3] Gi-Hyun Jeong and Han-Seon Lee, H. S. (2018). “Ground-motion prediction equation for South Korea based on recent earthquake records”. *Earthquake and Structures*, 15(1), 29-44.

[4] Korea Institute of Geoscience and Mineral Resources. https://www.kigam.re.kr/

[5] Kwang-Hee Kim, Jin-Han Ree, YoungHee Kim, Sungshil Kim, Su Young Kang and Wooseok Seo. (2018). “Assessing whether the 2017 M_w 5.4 Pohang earthquake in South Korea was an induced event”. *Science*, 360(6392), 1007-1009.

[6] Ministry of the Interior and Safety, Republic of Korea. https://www.mois.go.kr/eng/a01/engMain.do

[7] Architectural Institute of Korea - AIK(2016). *KBC2016 : Korean Building Code*. Prepared by the AIK., Seoul, Korea.

[8] Jeong SH. (2017). Summary of 2017 Pohang Earthquake (2017.11.15., M_w=5.4), 2017 Special Forum of EESK: Pohang earthquake and building damage: 2017 Nov 27; Seoul, Korea.

[9] Kobiz Media Co., Ltd. (2018). The Korea Bizwire. http://koreabizwire.com/what-if-major-earthquake-hits-seoul/101744

[10] Han-Seon Lee and Dong-Woo Ko. (2002). “Shaking table tests of a high RC bearing-wall structure with bottom piloti stories”. *Journal of Asian Architecture and Building Engineering*, 1(1), 47–54.

[11] DATAHUB.(2014).https://datacenterhub.org/

[12] Architectural Institute of Korea - AIK(2009). *KBC2009 : Korean Building Code*. Prepared by the AIK., Seoul, Korea.

[13] Kyung-Ran Hwang and Han-Seon Lee. (2018). “Seismic damage to RC low-rise building structures having irregularities at the ground story during the 15 November 2017 Pohang, Korea, earthquake”. *Journal of the Earthquake Engineering Society of Korea*, 22(3), 103-111.

[14] Computers & Structures, Inc. (2006). PERFORM Components and Elements for PERFORM-3D and PERFORM-Collaspse ver4. Computers & Structures, Inc., Berkeley, CA, USA. https://www.csiamerica.com/

[15] American Society of Civil Engineering. (2006). “ASCE/SEI 41-06”. Seismic Rehabilitation of Existing Building, Reston, VA.